Periodica Polytechnica
Civil Engineering

60(2), pp. 257–267, 2016
DOI: 10.3311/PPci.8884

RESEARCH ARTICLE

Natural Forest Regeneration Algorithm for Optimum Design of Truss Structures with Continuous and Discrete Variables

Hossein Moez, *Ali* Kaveh, *Nasser* Taghizadieh

Received 08-12-2015, accepted 17-12-2015

Abstract

In this paper the recently developed nature inspired meta-heuristic algorithm is utilized for optimum design of truss structures with continuous and discrete variables. This algorithm is inspired by the natural process happening in the forests with the rapidly change of environment and their natural regeneration. Based on this process a simple powerful optimization technique is introduced so-called Natural Forest Regeneration (NFR). Some well-studied benchmark structural problems are investigated with both continuous and discrete sizing variables and the results of the NRF are compared to those of some previously developed algorithms.

Keywords

truss optimum design · continuous variables · discrete variables · natural forest regeneration method · meta-heuristic algorithm · nature-inspired optimization

Hossein Moez
The Faculty of Civil Engineering, University of Tabriz, 5166416471, Tabriz, Iran

Ali Kaveh
Centre of Excellence for Fundamental Studies in Structural Engineering, Iran University of Science and Technology, Narmak, Tehran-16, Iran
e-mail: alikaveh@iust.ac.ir

Nasser Taghizadieh
The Faculty of Civil Engineering, University of Tabriz, 5166416471, Tabriz, Iran

1 Introduction

Optimal design of structures is one of the most active fields of structural engineering. Optimal design of structures is a non-linear programming problem and in the past the mathematical methods have been used for solution. Most of these methods are based on the gradient information to search the problem's space and a good starting point is needed to solve the problem. Though the gradient based methods produce accurate solutions and converge fast, however because of the costly achieved gradient information, the vital role of good starting point, and some other issues like the convexity and smoothness of search space, in recent years metaheuristic algorithms are used for optimal design of structures. Genetic Algorithm (GA) [1], Tabu Search [2], Ant Colony Optimization (ACO) [3], Particle Swarm Optimization (PSO) [4], Harmony Search (HS) [5], Big Bang-Big Crunch (BB-BC) [6], Charged System Search (CSS) [7], Magnetic Charged System Search (MCSS) [8], Ray optimization (RO) [9], Dolphin Echolocation Optimization (DEO) [10], Swallow Swarm Optimization (SSO) [11], Search group algorithm (SGA) [12], Colliding Bodies Optimization (CBO) [13] and Ant Lion Optimizer (ALO) [14] among other methods, are introduced and implemented in various structural design problems. Some successful applications of meta-heuristic algorithms can be found in the work of Refs. [15–18].

Recently a simple and powerful optimization algorithm, so-called Natural Forest Regeneration (NFR) is developed by the present authors for optimization problems, which mimics the natural migration of forests due to climate changes [19]. This population based algorithm is inspired by the natural behavior of the forests, against the rapidly changing environment. This phenomenon is combined with natural regeneration of forest. Exploration and exploitation aspects of the algorithm are achieved by seed dispersal mechanism and decreasing radius of seed dispersed area. The method is simple and easy to implement, and the optimized benchmark problems show the efficiency and robustness of the new algorithm.

Trusses are a well-known, extremely strong, cost effective option for the construction of diverse structures, especially for long spans and heavy loads. Therefore optimum design of trusses is widely investigated by researchers in recent decades. In the other hand, most of the optimization algorithms are first utilized for design of truss structures because of their simplicity. Optimal design of trusses can be categorized into three major classes: (i) Sizing optimization, where the cross sectional areas of the members are taken as optimization variables and the geometry of the structure is unchanged. (ii) Shape optimization, where the nodal coordinates are also taken as the optimization variables. (iii) Topology optimization, where the connections between nodes are added to the optimization variables.

In this paper, NFR is used for optimum design of truss structures with continuous and discrete variables and results are compared to those from the literature. The remainder of the paper is organized as follows: In Section 2 the method is briefly described. Three well-known benchmark structural problems are studied in Section 3. Finally, concluding remarks are presented in Section 4.

2 Natural forest regeneration algorithm

A possible fate for forest tree populations in a rapidly changing environment is persistence through migration to track ecological niches spatially. In the other hand, Forests are regenerated and redistributed naturally and the current location and population of forests are dependent on the environmental condition.

Forests can be regenerated manually by keeping seed trees and harvesting the other ones. Seed trees are the best looking ones and can be selected by comparing the trees. After the falling of the seeds on the ground and growing the seedlings, the process of keeping the best ones and harvesting others should be performed. Seed dispersal may be carried out by birds or water stream and this helps the forest to find new positions.

The migration of forests by seed dispersal and the process of keeping best trees and harvesting the others are two main ideas which are utilized here to design the new optimization algorithm. This algorithm is a population based algorithm and contains a guided random search. The main assumptions of the algorithm are:

- Each optimization candidate is represented by a tree.
- The height of a tree is considered to be proportional to its fitness.
- Each tree produces seeds and the number of seed dispersal of a tree is proportional to its height.
- The seeds are assumed to be dispersed around the trees.
- A portion of seeds are dispersed by the birds or water streams to far locations.
- After growing the seedlings, seed trees which are best ones, are kept and the others are harvested.

Using the above mentioned assumptions, the process of optimization can be presented by the following steps:

Step 1. Generate NT random trees in the feasible region of the side constraints of the problem.

Step 2. Calculate the objective function (obj) and the corresponding fitness (fit) for the j^{th} tree, and sort them in descending order. Fitness is defined as the inverse of the objective function and the height of the j^{th} tree,$h(j)$, is defined as its fitness.

$$h(j) = fit(j) = \frac{1}{obj(j) + \delta} \ , \quad j = 1, \ldots, NT \qquad (1)$$

where δ is a positive number to avoid the divide by zero error. For engineering design problems, the objective is positive, then $\delta = 0$ will not lead to error but for functions with zero or negative values, δ may become a dynamic parameter as follows:

$$\delta = |min(obj(j))| + \varepsilon \ , \quad j = 1, \ldots, NT \qquad (2)$$

where ε is a small positive number.

Step 3. Select NST best trees as seed trees and store them in **ST** and harvest the other ones.

Step 4. The j^{th} seed tree disperses $NS(j)$ seeds with random positions and $NS = (NT - NST)$ new seedlings will be produced. The number of seeds depends on the height of the seed tree.

The number of seeds of the i^{th} seed tree can be expressed by the following formula:

$$NS(j) = round(\frac{h(j)}{\sum_{i=1}^{NST} h(i)} NS) \qquad (3)$$

The positions of seeds are determined randomly:

$$\mathbf{XS}_i = \mathbf{X}_j + \mathbf{R}_i, i = 1, \ldots NS_j \qquad (4)$$

where $\mathbf{XS}_i$ is the position vector of the i^{th} seed and $\mathbf{X}_j$ is the position vector of the j^{th} seed tree and $\mathbf{R}_i$ is a random vector with negative or positive entries as:

$$\mathbf{R}_i = (rand \times 2 - 1)\, \mathbf{d} r_1 (1 - \frac{iter}{itermax}) \qquad (5)$$

$rand$ is a random number between 0.0 and 1.0, generated by the computer, $\mathbf{d}$ is a vector, containing the domains of the variables, and r_1 determines the region of the seeds around the seed tree, as a portion of the whole domain, and may be taken as $r_1 < 0.1$. Here, $itermax$ is the maximum number of iterations, determined by the user. Using the Eq. (5), the seed dispersal area will decrease linearly.

Step 5. Some seeds will be dispersed by birds or water streams. The new position of the seeds is defined as:

$$\mathbf{X}_{i,new} = \mathbf{X}_{i,old} + \mathbf{M}_i, i = 1, \ldots NM \qquad (6)$$

where $\mathbf{X}_{i,new}$ is the new position vector and $\mathbf{X}_{i,old}$ is the old position vector of the i^{th} seed respectively, and NM is the number of movements which is defined as part of all the seeds (20% is taken in this study) and $\mathbf{M}_i$ is the movement vector, with negative or positive entries, as follows:

$$\mathbf{M}_i = (rand \times 2 - 1)\, \mathbf{d} r_2 \qquad (7)$$

Here, $r_2 = 0.5$ is used.

Step 6. In the last two steps, some seeds may move of the boundaries of side constraints. One may use a fly-back mechanism to re-use one of the previous trees, which were in the allowed boundaries.

Step 7. Calculate the objective function and the corresponding fitness for each new seedling.

Step 8. If any of termination criterions is reached, stop the iteration, else go to Step 3.

Termination criterion may be selected from one of the following conditions or their combination:

1 Maximum number of iterations is reached.

2 Maximum number of iterations without any update of ST is reached.

The flowchart of the algorithm is presented in Fig. 1.

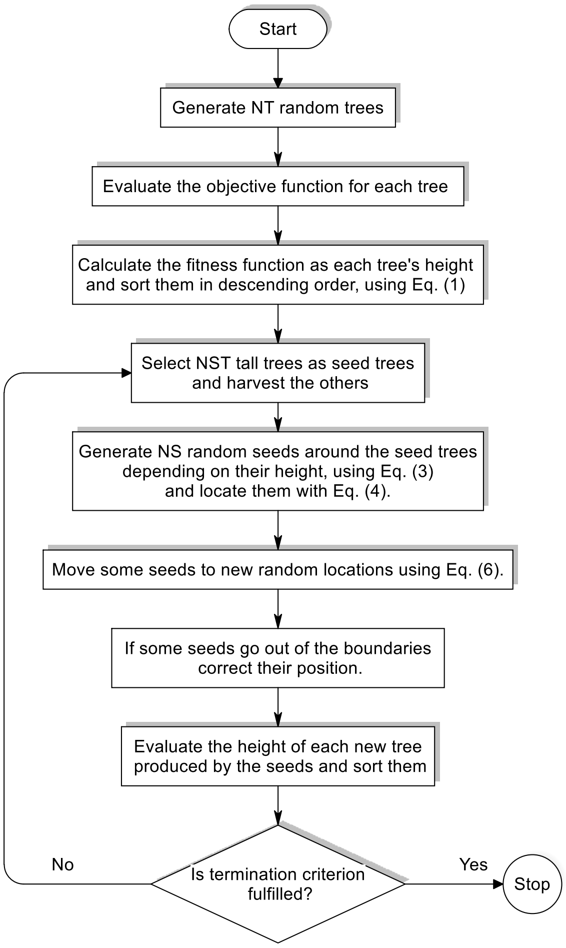

Fig. 1. The flowchart of the NFR.

3 Structural design examples

In this section, some benchmark truss design problems are studied and the results of the application of NFR are compared with those of the literature. All of the examples are studied with discrete and continuous sizing variables separately and for discrete form of the algorithm a simple rounding approach is utilized [20]. The main features and assumptions of the following examples are summarized in Table 1. It can be mentioned that in discrete problems, because of the exploration aspect of the algorithm, greater values for r_1 is used. In the other hand for larger problems (large number of structural members), due to the high computational time, the number of population and iterations are decreased. In the first example, the algorithm stops after 500 iterations without updating the seed trees. The other examples do not use this termination criterion and continue the iterations until reaching the maximum permitted iterations. The number of structural analyses is equal to the multiple of NT and $itermax$ for examples 2 and 3, while it is less than this values for the first example. The algorithm is coded in FORTRAN and the random generator function is taken from Numerical Recipes [21].

Optimum design of a truss structure with m members and ng groups of members is formulated as:

$$\begin{aligned} &\text{Find } \mathbf{X} = [x_1 x_2, \ldots, x_{ng}] \\ &\text{to minimize } Obj\,(\mathbf{X}) = \sum_{i=1}^{m} (\rho_i A_i(\mathbf{X}).l_i) \times Pen(\mathbf{X}) \end{aligned} \tag{8}$$

where $\mathbf{X}$ represents the vector of design variables, which includes the cross sectional areas of members in each group. $Obj(\mathbf{X})$ is the objective function, that consists of the weight of the structure multiplied by a penalty function $Pen(\mathbf{X})$, to convert a constrained structural optimization problem into an unconstrained one. ρ_i, l_i and A_i are the material density, length and cross section area of each structural member, respectively. The penalty function is defined as:

$$Pen\,(\mathbf{X}) = (1 + \varepsilon_1.q)^{\varepsilon_2} \tag{9}$$

For the comparison purpose, $\varepsilon_1 = 1.0$ and ε_2 is taken as 1.5 at the start of the iteration and increased to 6.0 linearly. q is the total amount of violations of constraints:

$$q = \sum_{i=1}^{m} \max\left(0, q_i^{strength}\right) + \max\left(0, q^{disp}\right) \tag{10}$$

where $q_i^{strength}$ and q^{disp} are the strength and displacement constraints violations, respectively. m denotes the number of members. These constraints can be defined using ASD-AISC code of practice [21].

3.1 A 10-bar planar truss

The 10-bar truss structure is a well-studied problem in the field of structural optimization which is used to verify the eficiency of a newly proposed optimization algorithms with continuous or discrete variables [22,23].

Fig. 2 shows the geometry and support conditions of this 2D cantilevered truss with loading condition. The material density is 0.1 lb/in^3 (2767.990 kg/m^3) and the modulus of elasticity is 10,000 ksi (68,950 MPa). The members are subjected to the stress limits of 25 ksi (172.375 MPa) and all the nodes in both

Tab. 1. NFR assumptions for benchmark truss optimization problems

Example No.	Variables type	n	m	ng	r_1	r_2	NT	NST	$itermax$
1	Continuous	6	10	10	0.01	0.3	50	5	3000
	Discrete	6	10	10	0.1	0.3	50	5	2000
2	Continuous	20	72	16	0.01	0.3	50	5	200
	Discrete	20	72	16	0.1	0.3	20	5	200
3	Continuous	153	582	32	0.001	0.5	20	3	400
	Discrete	153	582	32	0.01	0.5	20	3	400

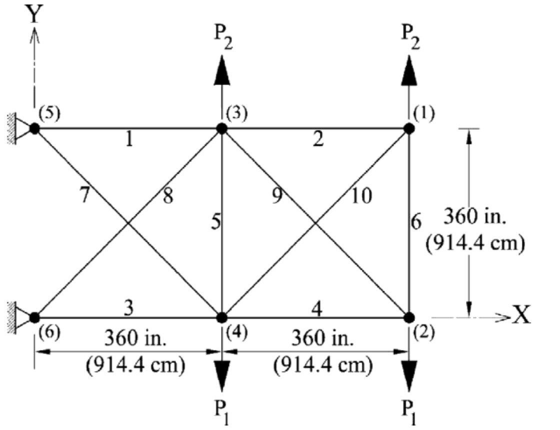

Fig. 2. Schematic of the 10-bar planar truss structure.

vertical and horizontal directions are subjected to the displacement limits of 2.0 in (5.08 cm). In this example, there are 10 design variables and is studied with both continuous and discrete variables.

In the first case, the continuous variables are used and a set of pseudo variables ranging from 0.1 to 35.0 in^2 (0.6452 cm^2 to 225.806 cm^2) are assumed. Here, two load cases are considered:

Load Case 1: P_1 = 100 kips (444.8 kN) and P_2 = 0,

Load Case 2: P_1 = 150 kips (667.2 kN) and P_2 = 50 kips (222.4 kN).

Comparisons of the results of the NFR with the previously published results using continuous variables are summarized in Table 2 and Table 3 for each load cases. As it can be seen from the tables, the best feasible result is obtained by HS algorithm for both load cases and among the other algorithms, only PSOPC and HPSO found better results than NFR in 150000 analyses. Where the NFR finds the best result after 62950 and 108100 analyses for the load Case 1 and load Case 2 respectively. As it can be observed from Tables 2 and 3 that the best weights obtained using NFR in both cases are only slightly bigger than the HPSACO.

In the second case, the discrete variables are selected from the set D = {0.1, 0.5, 1.0, 1.5, 2.0, 2.5, 3.0, 3.5, 4.0, 4.5, 5.0, 5.5, 6.0, 6.5, 7.0, 7.5, 8.0, 8.5, 9.0, 9.5, 10.0,10.5, 11.0, 11.5, 12.0, 12.5, 13.0, 13.5, 14.0, 14.5, 15.0, 15.5, 16.0, 16.5, 17.0, 17.5, 18.0, 18.5, 19.0, 19.5, 20.0, 20.5, 21.0, 21.5, 22.0, 22.5, 23.0, 23.5, 24.0, 24.5, 25.0, 25.5, 26.0, 26.5, 27.0, 27.5, 28.0, 28.5, 29.0, 29.5, 30.0, 30.5, 31.0, 31.5}(in^2) and the load Case 1 is applied to the truss. Table 4 summarizes the comparison between previously published results and the results of the NFR with discrete variables. Comparing the results shows that the branch and bound method reached the best feasible result, and the other methods have slightly larger optimum result compared to NFR.

3.2 A 72-bar space truss

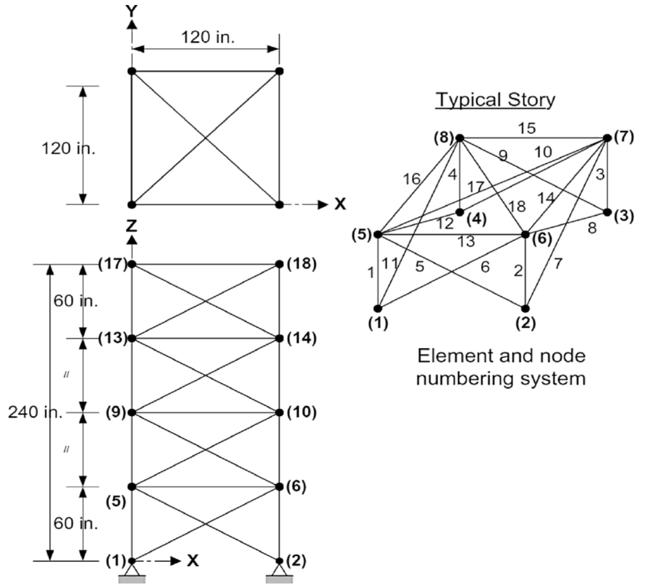

Fig. 3. Schematic of a 72-barspatial truss.

A 72-bar space truss with schematic shown in Fig. 3 is studied as the second example. This example is investigated by the researchers with continuous and discrete variables as well. 72 structural members of this spatial truss are categorized into 16 groups using symmetry:

((1) A1–A4, (2) A5–A12, (3) A13–A16, (4) A17–A18, (5) A19–A22, ((6)A23–A30, (7) A31–A34, (8) A35–A36, (9) A37–A40, (10) A41–A48, (8) A49–A52, (9) A53–A54, (13) A55–A58, (14) A59–A66 (15), A67–A70, and (16) A71–A72.

The material density is 0.1 lb/in.^{3} (2767.990 kg/m^3) and the modulus of elasticity is taken as 10,000 ksi (68,950 MPa). The members are subjected to the stress limits of ±25 ksi (±172.375 MPa). The uppermost nodes are subjected to the displacement limits of ±0.25 in (±0.635 cm) in both x and y direc-

Tab. 2. Comparison of the NFR results for the 10-bar truss with those of the literature using continuous variables (Load Case 1)

Element group		Camp et al. [24]	Lee and Geem [29]	Li et al. [26]			Kaveh and Talatahari [32]	Kaveh et al.[28]		Present work
		GA	HS	PSO	PSOPC	HPSO	HPSACO	MCSS	IMCSS	NFR
1	A1	28.92	30.15	33.469	30.569	30.704	30.307	29.5766	30.0258	30.6206
2	A2	0.1	0.102	0.11	0.1	0.1	0.1	0.1142	0.1	0.1058
3	A3	24.07	22.71	23.177	22.974	23.167	23.434	23.8061	23.6277	23.1368
4	A4	13.96	15.27	15.475	15.148	15.183	15.505	15.8875	15.9734	15.3435
5	A5	0.1	0.102	3.649	0.1	0.1	0.1	0.1137	0.1	0.1017
6	A6	0.56	0.544	0.116	0.547	0.551	0.5241	0.1003	0.5167	0.5517
7	A7	7.69	7.541	8.328	7.493	7.46	7.4365	8.6049	7.4567	7.5205
8	A8	21.95	21.56	23.34	21.159	20.978	21.079	21.6823	21.4374	21.0745
9	A9	22.09	21.45	23.014	21.556	21.508	21.229	20.3033	20.7443	21.3645
10	A10	0.1	0.1	0.19	0.1	0.1	0.1	0.1117	0.1	0.1
Weight (lb)		5076.31	5057.88	5529.5	5061	5060.92	5056.56	5086.9	5064.6	5063.58
No. of analyses		N/A	20,000	150,000	150,000	N/A	10,650	8875	8475	62950

Tab. 3. Comparison of the NFR results for the 10-bar truss with those of the literature using continuous variables (Load Case 2)

Element group		Lee and Geem [25]	Li et al. [26]			Kaveh and Talatahari [27]	Kaveh et al. [28]		Present work
		HS	PSO	PSOPC	HPSO	HPSACO	MCSS	IMCSS	NFR
1	A1	23.25	22.935	23.473	23.353	23.194	22.863	23.299	23.33621
2	A2	0.102	0.113	0.101	0.1	0.1	0.12	0.1	0.1
3	A3	25.73	25.355	25.287	25.502	24.585	25.719	25.682	25.7048
4	A4	14.51	14.373	14.413	14.25	14.221	15.312	14.51	14.5081
5	A5	0.1	0.1	0.1	0.1	0.1	0.101	0.1	0.1
6	A6	1.977	1.99	1.969	1.972	1.969	1.968	1.969	1.9698
7	A7	12.21	12.346	12.362	12.363	12.489	12.31	12.149	12.2653
8	A8	12.61	12.923	12.694	12.894	12.925	12.934	12.36	12.6900
9	A9	20.36	20.678	20.323	20.356	20.952	19.906	20.869	20.3477
10	A10	0.1	0.1	0.103	0.101	0.101	0.1	0.1	0.1
Weight (lb)		4668.81	4679.47	4677.7	4677.29	4675.78	4686.47	4679.15	4677.43
No. of analyses		N/A	150,000	150,000	N/A	9625	7350	6625	108100

Tab. 4. Comparison of the NFR results for the 10-bar truss with those of the literature using discrete variables (Load Case 1)

Element group		Wu and Chow [29]	Ringertz [23]	Li et al. [26]			Present work
		SSGAs	Branch and Bound	PSO	PSOPC	HPSO	NFR
1	A1	30.5	30.5	24.5	25.5	31.5	30.0
2	A2	0.5	0.1	0.1	0.1	0.1	0.1
3	A3	16.5	23	22.5	23.5	24.5	24.
4	A4	15	15.5	15.5	18.5	15.5	14.5
5	A5	0.1	0.1	0.1	0.1	0.1	0.1
6	A6	0.1	0.5	1.5	0.5	0.5	0.5
7	A7	0.5	7.5	8.5	7.5	7.5	7.5
8	A8	18	21	21.5	21.5	20.5	21.0
9	A9	19.5	21.5	27.5	23.5	20.5	22.0
10	A10	0.5	0.1	0.1	0.1	0.1	0.1
Weight (lb)		4217.3	5059.9	5243.71	5133.16	5073.51	5067.33

tions. The loading conditions are considered as:

Load condition 1. Loads 5, 5 and 5 kips in the x, y and z directions at node 17, respectively.

Load condition 2. A load 5 kips in the z direction at nodes 17, 18, 19 and 20.

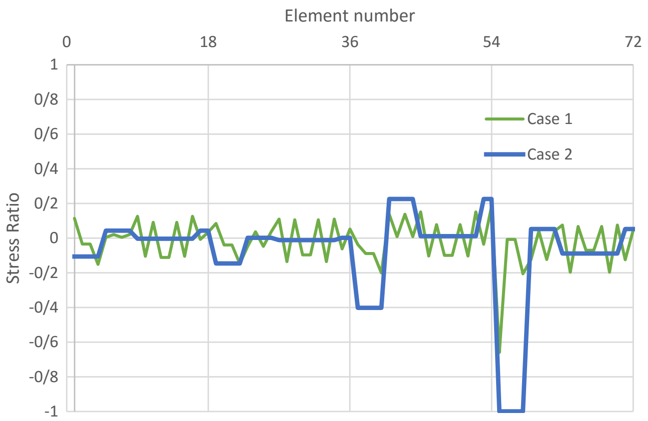

Fig. 4. Comparison of the allowable and existing stresses in the elements of the 72-bar truss structure with continuous variables

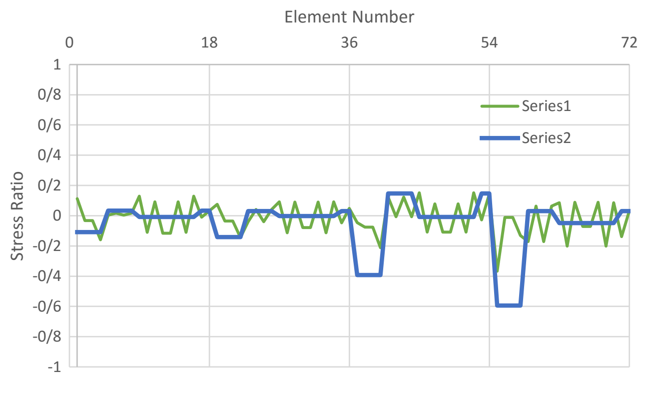

Fig. 5. Comparison of the allowable and existing stresses in the elements of the 72-bar truss structure with discrete variables.

In the continuous sizing variables case, the minimum and maximum permitted cross-sectional area of each member is taken as 0.10 in^2 (0.6452 cm^2) and 4.00 in^2 (25.81 cm^2) respectively. Table 5 summarizes the results obtained by the present work and those of the previously reported researches. The best result of the NFR approach is 379.9248, while it is 385.76, 380.24, 381.91, 379.85, 380.458 and 379.6943 lb for the GA [30], ACO [31], PSO [32], BB–BC [33] RO [9], CBO [34], respectively As it can be seen from the table, the best feasible result is obtained by BB-BC algorithm but NFR achieves a comparable result with less number of structural analyses. Fig. 4 shows the allowable and existing stress values in truss member using the NFR

This problem is solved again with discrete variables and these variables are selected from the set D = {0.1, 0.2, 0.3, 0.4, 0.5, 0.6, 0.7, 0.8, 0.9, 1.0, 1.1, 1.2, 1.3, 1.4, 1.5, 1.6, 1.7,1.8, 1.9, 2.0, 2.1, 2.2, 2.3, 2.4,2.5, 2.6, 2.7, 2.8, 2.9, 3.0, 3.1, 3.2}(in^2) or {0.65, 1.29, 1.94, 2.58, 3.23, 3.87, 4.52, 5.16, 5.81, 6.45,7.10, 7.74, 8.39, 9.03, 9.68, 10.32, 10.97, 12.26, 12.90, 13.55, 14.19,14.84, 15.48, 16.13, 16.77, 17.42, 18.06, 18.71, 19.36, 20.00, 20.65}(cm^2). The comparison of the results of the optimized discrete cross sections of the 72-bar truss with the previously published results is presented in Table 6. The best optimized weight of the NFR algorithm is equal to 386.95 lb (175.52 kg) and it is comparable to the best weight of the IM-CSS and DHPSACO algorithm which is equal to 385.54 lb (174.88 kg), while it is 389.49 lb 388.94 lb, 387.94 lb, 400.66 lb for the MCSS, HPSO, HS, and GA, respectively.

In this example, because of the effect of the utilized rounding method and smaller number of populations in discrete form of the problem, the NFR produced better results with continuous variables.

By comparing Fig. 4 and Fig. 5, it can be seen that in discrete sizing variables case, the stress ratio has not reach the maximum value of unity and thus the weight of the structure is increased compared to the continuous sizing variables case.

3.3 A 582-bar tower truss

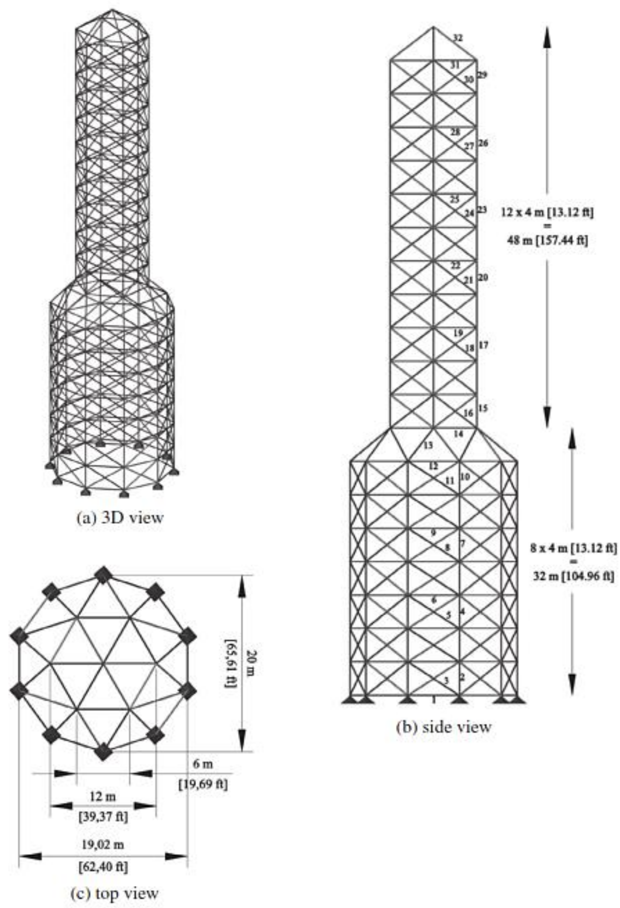

Fig. 6. Schematic of 582-bar tower truss and element numbering.

The 582-bar spatial truss structure shown in Fig. 6 has been studied by the researchers [13,36,37]. This structure is designed both with discrete and continuous sizing variables. Due to structural symmetry, the 582 members are categorized as 32 independent size variables as shown in Fig. 6. A single load case is

Tab. 5. Comparison of the NFR results for the 72-bar to those of the literature with continuous variables

Element Group		Erbatur et al. [30]	Camp et al. [31]	Perez et al. [32]	Camp [33]	Kaveh et al. [9]	Kaveh et al. [34]	Present work
		GA	ACO	PSO	BB–BC	RO	CBO	NFR
1	A1–A4	1.755	1.948	1.7427	1.8577	1.8365	1.9028	1.8458
2	A5–A12	0.505	0.508	0.5185	0.5059	0.5021	0.518	0.5162
3	A13–A16	0.105	0.101	0.1	0.1	0.1	0.1001	0.1000
4	A17–A18	0.155	0.102	0.1	0.1	0.1004	0.1003	0.1000
5	A19–A22	1.155	1.303	1.3079	1.2476	1.2522	1.2787	1.3280
6	A23–A30	0.585	0.511	0.5193	0.5269	0.5033	0.5074	0.4992
7	A31–A34	0.1	0.101	0.1	0.1	0.1002	0.1003	0.1000
8	A35–A36	0.1	0.1	0.1	0.1012	0.1001	0.1003	0.1036
9	A37–A40	0.46	0.561	0.5142	0.5209	0.573	0.524	0.5092
10	A41–A48	0.53	0.492	0.5464	0.5172	0.5499	0.515	0.5187
11	A49–A52	0.12	0.1	0.1	0.1004	0.1004	0.1002	0.1002
12	A53–A54	0.165	0.107	0.1095	0.1005	0.1001	0.1015	0.1016
13	A55–A58	0.155	0.156	0.1615	0.1565	0.1576	0.1564	0.1565
14	A59–A66	0.535	0.55	0.5092	0.5507	0.5222	0.5494	0.5463
15	A67–A70	0.48	0.39	0.4967	0.3922	0.4356	0.4029	0.4316
16	A71–A72	0.52	0.592	0.5619	0.5922	0.5971	0.5504	0.5597
Best weight (lb)		386.4435	380.2387	381.9363	379.8404	380.4505	379.6943	379.9248
Average weight (lb)		N/A	383.16	N/A	382.08	382.553	379.8961	380.2061
Stddev		N/A	3.66	N/A	1.912	1.221	0.0791	0.3808
Number of structural analyses		N/A	18,500	N/A	19,621	19,084	15,600	10,000

Tab. 6. Comparison of the NFR results for the 72-bar truss to those of the literature with discrete variables

Element Group		Wu and Chow [29]	Lee and Geem [25]	Li et al. [35]			Kaveh and Talatahari [27]	Kaveh et al. [28]		Present Work
		GA	HS	PSO	PSOPC	HPSO	DHPSACO	MCSS	IMCSS	NFR
1	A1–A4	1.5	1.9	2.6	3	2.1	1.9	1.8	2	2.0
2	A5–A12	0.7	0.5	1.5	1.4	0.6	0.5	0.5	0.5	0.5
3	A13–A16	0.1	0.1	0.3	0.2	0.1	0.1	0.1	0.1	0.1
4	A17–A18	0.1	0.1	0.1	0.1	0.1	0.1	0.1	0.1	0.1
5	A19–A22	1.3	1.4	2.1	2.7	1.4	1.3	1.3	1.3	1.3
6	A23–A30	0.5	0.6	1.5	1.9	0.5	0.5	0.5	0.5	0.5
7	A31–A34	0.2	0.1	0.6	0.7	0.1	0.1	0.1	0.1	0.1
8	A35–A36	0.1	0.1	0.3	0.8	0.1	0.1	0.1	0.1	0.1
9	A37–A40	0.5	0.6	2.2	1.4	0.5	0.6	0.7	0.5	0.5
10	A41–A48	0.5	0.5	1.9	1.2	0.5	0.5	0.6	0.5	0.5
11	A49–A52	0.1	0.1	0.2	0.8	0.1	0.1	0.1	0.1	0.1
12	A53–A54	0.2	0.1	0.9	0.1	0.1	0.1	0.1	0.1	0.1
13	A55–A58	0.2	0.2	0.4	0.4	0.2	0.2	0.2	0.2	0.2
14	A59–A66	0.5	0.5	1.9	1.9	0.5	0.6	0.6	0.6	0.6
15	A67–A70	0.5	0.4	0.7	0.9	0.3	0.4	0.4	0.4	0.5
16	A71–A72	0.7	0.6	1.6	1.3	0.7	0.6	0.4	0.6	0.5
Weight (kg)		400.66	387.94	1089.88	1069.79	388.94	385.54	389.49	385.54	386.95
Number of structural analyses		N/A	N/A	N/A	150,000	50,000	5330	5400	3625	4000

Tab. 7. Optimum design cross-sections for the 582-bar tower truss with continuous variables

Element groups	Kaveh et al. (CBO) [32] Area (cm^2)	Present work (NFR) Area (cm^2)
1	20.5226	20.3628
2	162.7709	159.3532
3	24.8562	24.3983
4	122.7462	123.5066
5	21.6756	20.4200
6	21.4751	20.4167
7	110.8568	109.9024
8	20.9355	22.3195
9	23.1792	20.5380
10	109.6085	109.6124
11	21.2932	20.3442
12	156.2254	156.7294
13	159.3948	160.6597
14	107.3678	106.8843
15	171.9150	170.8052
16	31.5471	29.4508
17	155.6601	153.9078
18	21.4951	22.5768
19	25.1163	23.5369
20	94.0228	93.8706
21	20.8041	21.5362
22	21.2230	20.4411
23	53.5946	52.6982
24	20.6280	20.8369
25	21.5057	20.2627
26	26.2735	25.1554
27	20.6069	20.7636
28	21.5076	21.2053
29	24.1394	24.2208
30	20.2735	21.5632
31	21.1888	22.9673
32	29.6669	27.7757
Volume (m^3)	16.1520	16.0204
Number of structural analyses	20000	8000

considered consisting of lateral loads of 5.0 kN (1.12 kips) applied in both x- and y-directions and a vertical load of 30 kN (6.74 kips) applied in the negative z-direction at all nodes of the tower.

The allowable tensile and compressive stresses are used according to the AISC-ASD [38] code, as follows:

$$\begin{cases} \sigma_i^+ = 0.6F_y \text{ for } \sigma_i > 0.0 \\ \sigma_i^- \text{ for } \sigma_i < 0.0 \end{cases} \tag{11}$$

where σ_i^- is calculated according to slenderness ratio:

$$\begin{aligned} \sigma_i^- &= \begin{cases} \left[\left(1 - \frac{\lambda_i^2}{2C_c^2}\right)F_y\right] \Big/ \left(\frac{5}{3} + \frac{3}{8}\frac{\lambda_i}{C_c} - \frac{\lambda_i^3}{8C_c^3}\right) \text{ for } \lambda_i < C_c \\ \frac{12}{23}\frac{\pi^2 E}{\lambda_i^2} \text{ for } \lambda_i \geq C_c \end{cases} \\ \lambda_i &= \frac{kl_i}{r_i} \\ C_c &= \sqrt{2\pi^2} \Big/ F_y \end{aligned} \tag{12}$$

where E is the modulus of elasticity, F_y is the yield stress of steel, λ_i is the slenderness ratio, with k being the effective length factor, l_i is the member length and r_i is the radius of gyration.C_c is the slenderness ratio dividing the elastic and inelastic buckling regions.

The maximum slenderness ratio is limited to 300 for tension members, and it is recommended to be limited to 200 for compression members according to ASD-AISC [36]. The modulus of elasticity is 29,000 ksi (203893.6 MPa) and the yield stress of steel is taken as 36 ksi (253.1 MPa). Other constraints are the limitations of nodal displacements which should be no more than 8.0 cm (3.15 in.) in all directions.

In the case of continuous sizing variables, the lower and upper bounds of size variables are taken as 3.1 in.^{2} (20 cm^2) and 155.0 in.^{2}(1000 cm^2), respectively. The radius of gyration r_i, can be expressed in terms of cross-sectional areas, i.e., $r_i = aA_i^b$ [39]. Here, a and b are the constants depending on the types of sec-

Tab. 8. Optimum design cross-sections for the 582-bar tower truss with discrete variables

Element Groups	Hasançebi et al. [40] (PSO)			Kaveh et al. [36](DHPSACO)			Kaveh et al. [20] (CBO)			Present work (NFR)		
	Ready Section	Area (cm^2)	Area (in^2)	Ready Section	Area (cm^2)	Area (in^2)	Ready Section	Area (cm^2)	Area (in^2)	Ready Section	Area (cm^2)	Area (in^2)
1	W8X21	39.74	(6.16)	W8X24	45.68	(7.08)	W8X21	39.74	(6.16)	W8X24	45.68	7.08
2	W12X79	149.68	(23.2)	W12X72	136.13	(21.1)	W12X79	149.68	(23.20)	W12X72	136.13	21.10
3	W8X24	45.68	(7.08)	W8X28	53.16	(8.24)	W8X28	53.22	(8.25)	W6X25	47.35	7.34
4	W10X60	113.55	(17.08)	W12X58	109.68	(17)	W10X60	90.96	(14.10)	W10X60	114.19	17.70
5	W8X24	45.68	(7.08)	W8X24	45.68	(7.08)	W8X24	45.68	(7.08)	W8X24	45.68	7.08
6	W8X21	39.74	(6.16)	W8X24	45.68	(7.08)	W8X21	39.74	(6.16)	W8X24	45.68	7.08
7	W8X48	90.97	(14.1)	W10X49	92.90	(14.4)	W10X68	128.38	(19.90)	W12X50	94.19	14.60
8	W8X24	45.68	(7.08)	W8X24	45.68	(7.08)	W8X24	45.68	(7.08)	W8X24	45.68	7.08
9	W8X21	39.74	(6.16)	W8X24	45.68	(7.08)	W8X21	39.74	(6.16)	W8X24	45.68	7.08
10	W10X45	85.81	(13.3)	W12X40	75.48	(11.7)	W14X48	90.96	(14.10)	W8X40	75.48	11.70
11	W8X24	45.68	(7.08)	W12X30	56.71	(8.79)	W12X26	49.35	(7.65)	W6X25	47.35	7.34
12	W10X68	129.03	(20)	W12X72	136.129	(21.1)	W21X62	118.06	(18.30)	W10X68	128.39	19.90
13	W14X74	140.65	(21.8)	W18X76	143.87	(23.3)	W18X76	143.87	(22.30)	W14X74	140.64	21.80
14	W8X48	90.97	(14.1)	W10X49	92.90	(14.4)	W12X53	100.64	(15.60)	W14X48	90.97	14.10
15	W18X76	143.87	(22.3)	W14X82	154.84	(24)	W14X61	115.48	(17.90)	W27X84	159.35	24.70
16	W8X31	55.90	(9.13)	W8X31	58.84	(9.12)	W8X40	75.48	(11.70)	W8X31	58.90	9.13
17	W8X21	39.74	(6.16)	W14X61	115.48	(17.9)	W10X54	101.93	(15.80)	W18X76	143.87	22.30
18	W16X67	127.10	(19.7)	W8X24	45.68	(7.08)	W12X26	49.35	(7.65)	W8X24	45.68	7.08
19	W8X24	45.68	(7.08)	W8X21	39.74	(6.16)	W8X21	39.74	(6.16)	W8X21	39.74	6.16
20	W8X21	39.74	(6.16)	W12X40	75.48	(11.7)	W14X43	81.29	(12.60)	W10X45	85.81	13.30
21	W8X40	75.48	(11.7)	W8X24	45.68	(7.08)	W8X24	45.68	(7.08)	W8X24	45.68	7.08
22	W8X24	45.68	(7.08)	W14X22	41.87	(6.49)	W8X21	39.74	(6.16)	W10X22	41.87	6.49
23	W8X21	39.74	(6.16)	W8X31	58.84	(9.12)	W10X22	41.87	(6.49)	W8X21	39.74	6.16
24	W10X22	41.87	(6.49)	W8X28	53.16	(8.24)	W8X24	45.68	(7.08)	W12X26	49.35	7.65
25	W8X24	45.68	(7.08)	W8X21	39.74	(6.16)	W8X21	39.74	(6.16)	W8X21	39.74	6.16
26	W8X21	39.74	(6.16)	W8X21	39.74	(6.16)	W8X21	39.74	(6.16)	W8X21	39.74	6.16
27	W8X21	39.74	(6.16)	W8X24	45.68	(7.08)	W8X24	45.68	(7.08)	W8X21	39.74	6.16
28	W8X24	45.68	(7.08)	W8X28	53.16	(8.24)	W8X21	39.74	(6.16)	W8X24	45.68	7.08
29	W8X21	39.74	(6.16)	W16X36	68.39	(10.6)	W8X21	39.74	(6.16)	W12X26	49.35	7.65
30	W8X21	39.74	(6.16)	W8X24	45.68	(7.08)	W6X25	47.35	(7.34)	W10X33	62.65	9.71
31	W8X24	45.68	(7.08)	W8X21	39.74	(6.16)	W10X33	62.64	(9.71)	W8X24	45.68	7.08
32	W8X24	45.68	(7.08)	W8X24	45.68	(7.08)	W8X28	53.22	(8.25)	W8X21	39.74	6.16
Volume, m^3, (in^3)	22.3958 (1366674.89)			22.0607 (1346227.65)			21.8376 (1332612.11)			21.8151 (1331238.27)		
Number of structural analyses	50000			8500			6400			8000		

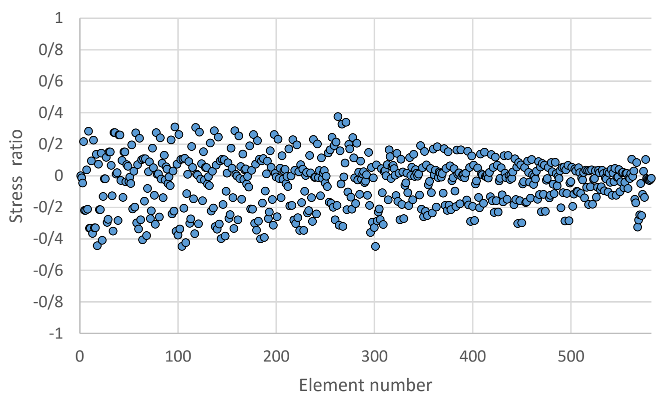

Fig. 7. Stress ratio in elements of the 582-bar truss with continous design variables.

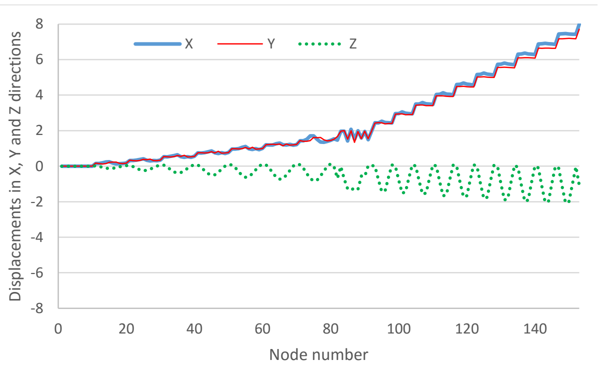

Fig. 8. Nodal displacements in X, Y and Z directions of the 582-bar truss with continous design variables.

tions adopted for the members such as pipes, angles, and tees. In this example, pipe sections (a = 0.4993 and b = 0.6777) were used for bars. Table 7 lists the optimal values of the 32 size variables obtained by the present algorithm and a comparison with the previously published results. It is obvious that the NFR achieved better result than CBO with less number of structural analyses Fig. 7 shows the allowable and existing stress ratio and displacement values of the NFR. The displacements of nodes are summarized in Fig. 8. Figs. 7 and 8 show that the displacement controls the design and the stress is not determinative.

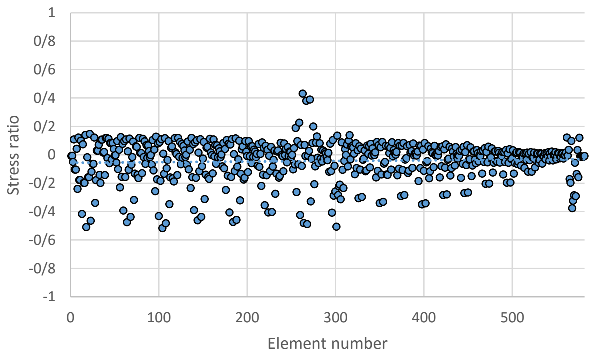

Fig. 9. Stress ratio in elements of the 582-bar truss wioth discrete design variables.

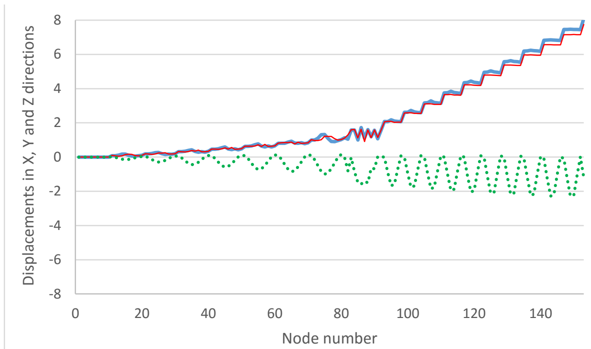

Fig. 10. Nodal displacements in X, Y and Z directions of the 582-bar truss with discrete design variables.

In the case of discrete sizing variables, design variables were selected from a discrete set of 137 standard steel W-shaped sections based on the area and radii of gyration of the sections [40]. Design variables can range between 6.16 in.^{2} (39.74) and 215 in.^{2} (1387.09 cm^2). Comparison of the optimal values of the 32 size variables with those of literature are listed in Table 8 It is clear that NFR reached the best solution and the number of structural analysis for NFR is comparable with the minimum value of the CBO method. Stress ratio in the elements of 582-bar truss with discrete design variables is presented in Fig. 9 and the nodal displacements for this case are summarized in Fig. 10.

4 Conclusions

The application of the recently developed methaheuristic algorithm, called as Natural Forest Regeneration, is extended in this paper for optimal design of truss structures. The presented algorithm is simple and easy to implement and comparable results are obtained by its use. Three benchmark truss structures are studied here with discrete and continous sizing variables. Comparison of the results with those of the previously published results, show that the NFR achieves comparable solution in most of the cases.

References

1 **Holland J H**, *Adaptation in natural and artificial systems: An introductory analysis with applications to biology, control, and artificial intelligence*, Michigan University Press, 1975.

2 **Glover F**, *Future paths for integer programming and links to artificial intelligence*, Computers & Operations Research, **13**(5), (1986), 533–549, DOI 10.1016/0305-0548(86)90048-1.

3 **Dorigo M**, *Optimization, learning and natural algorithms*, Ph.D. Thesis, Politecnico di Milano, Italy, 1992.

4 **Kennedy J**, *Particle swarm optimization, in Encyclopedia of Machine Learning*, Springer, 2010.

5 **Geem Z W, Kim J H, Loganathan G**, *A New Heuristic Optimization Algorithm: Harmony Search*, SIMULATION, **76**(2), (2001), 60–68, DOI 10.1177/003754970107600201.

6 **Erol O K, Eksin I**, *A new optimization method: Big Bang–Big Crunch*, Advances in Engineering Software, **37**(2), (2006), 106–111, DOI 10.1016/j.advengsoft.2005.04.005.

7 **Kaveh A, Talatahari S**, *A novel heuristic optimization method: charged system search*, Acta Mechanica, **213**(3-4), (2010), 267–289, DOI 10.1007/s00707-009-0270-4.

8 **Kaveh A, Motie Share M A, Moslehi M**, *Magnetic charged system search: a new meta-heuristic algorithm for optimization*, Acta Mechanica, **224**(1), (2013), 85–107, DOI 10.1007/s00707-012-0745-6.

9 **Kaveh A, Khayatazad M**, *A new meta-heuristic method: Ray Optimization*, Computers & Structures, **112-113**, (2012), 283–294, DOI 10.1016/j.compstruc.2012.09.003.

10 **Kaveh A, Farhoudi N**, *A new optimization method: Dolphin echolocation*, Advances in Engineering Software, **59**, (2013), 53–70, DOI 10.1016/j.advengsoft.2013.03.004.

11 **Kaveh A, Mahdavi V R**, *Colliding bodies optimization: A novel meta-heuristic method*, Computers & Structures, **139**, (2014), 18–27, DOI 10.1016/j.compstruc.2014.04.005.

12 **Neshat M, Sepidnam G, Sargolzaei M**, *Swallow swarm optimization algorithm: a new method to optimization*, Neural Computing and Applications, **23**(2), (2013), 429–454, DOI 10.1007/s00521-012-0939-9.

13 **Gonçalves M S, Lopez R H, Miguel L F F**, *Search group algorithm: A new metaheuristic method for the optimization of truss structures*, Computers & Structures, **153**, (2015), 165–184, DOI 10.1016/j.compstruc.2015.03.003.

14 **Mirjalili S**, *The Ant Lion Optimizer*, Advances in Engineering Software, **83**, (2015), 80–98, DOI 10.1016/j.advengsoft.2015.01.010.

15 **Csébfalvi A**, *Angel method for discrete optimization problems*, Periodica Polytechnica Civil Engineering, **51**(2), (2007), 37–46, DOI 10.3311/pp.ci.2007-2.06.

16 **Csébfalvi A**, *A hybrid meta-heuristic method for continuous engineering optimization*, Periodica Polytechnica Civil Engineering, **53**(2), (2009), 93–100, DOI 10.3311/pp.ci.2009-2.05.

17 **Kaveh A, Zolghadr A**, *A multi-set charged system search for truss optimization with variables of different natures; element grouping*, Periodica Polytechnica Civil Engineering, **55**(2), (2011), 87–98, DOI 10.3311/pp.ci.2011-2.01.

18 **Kaveh A, Javadi S M**, *An efficient hybrid particle swarm strategy, ray optimizer, and harmony search algorithm for optimal design of truss struc-*

tures, Periodica Polytechnica Civil Engineering, **58**(2), (2014), 155–171, DOI 10.3311/PPci.7550.

19 **Moez H, Kaveh A, Taghizadieh N**, *A novel meta-heuristic optimization algorithm: Natural forest regeneration algorithm*, Advances in Engineering Software, (2015). (submitted for publication).

20 **Kaveh A, Mahdavi V R**, *Colliding Bodies Optimization method for optimum discrete design of truss structures*, Computers & Structures, **139**, (2014), 43–53, DOI 10.1016/j.compstruc.2014.04.006.

21 **Press W H**, *Numerical recipes 3rd edition: The art of scientific computing*, Cambridge University Press, 2007.

22 **Rajeev S, Krishnamoorthy C S**, *Discrete Optimization of Structures Using Genetic Algorithms*, Journal of Structural Engineering, **118**(5), (1992), 1233–1250, DOI 10.1061/(ASCE)0733-9445(1992)118:5(1233).

23 **Ringertz UT**, *On methods for discrete structural optimization*, Engineering Optimization, **13**(1), (1988), 47–64, DOI 10.1080/03052158808940946.

24 **Camp C, Pezeshk S, Cao G**, *Optimized Design of Two-Dimensional Structures Using a Genetic Algorithm*, Journal of Structural Engineering, **124**(5), (1988), 551–559, DOI 10.1061/(ASCE)0733-9445(1998)124:5(551).

25 **Lee K S, Geem Z W**, *A new structural optimization method based on the harmony search algorithm*, Computers & Structures, **82**(9-10), (2004), 781–798, DOI 10.1016/j.compstruc.2004.01.002.

26 **Li L J, Huang Z B, Liu F**, *A heuristic particle swarm optimization method for truss structures with discrete variables*, Computers & Structures, **87**(7-8), (2009), 435–443, DOI 10.1016/j.compstruc.2009.01.004.

27 **Kaveh A, Talatahari S**, *Particle swarm optimizer, ant colony strategy and harmony search scheme hybridized for optimization of truss structures*, Computers & Structures, **87**(5-6), (2009), 267–283, DOI 10.1016/j.compstruc.2009.01.003.

28 **Kaveh A, Mirzaei B, Jafarvand A**, *An improved magnetic charged system search for optimization of truss structures with continuous and discrete variables*, Applied Soft Computing, **28**, (2015), 400–410, DOI 10.1016/j.asoc.2014.11.056.

29 **Wu S-J, Chow P-T**, *Steady-state genetic algorithms for discrete optimization of trusses*, Computers & Structures, **56**(6), (1995), 979–991, DOI 10.1016/0045-7949(94)00551-D.

30 **Erbatur F, Hasançebi O, Tütüncü İ, Kılıç H**, *Optimal design of planar and space structures with genetic algorithms*, Computers & Structures, **75**(2), (2000), 209–224, DOI 10.1016/S0045-7949(99)00084-X.

31 **Camp C V, Bichon B J**, *Design of Space Trusses Using Ant Colony Optimization*, Journal of Structural Engineering, **130**(5), (2004), 741–751, DOI 10.1061/(ASCE)0733-9445(2004)130:5(741).

32 **Perez R E, Behdinan K**, *Particle swarm approach for structural design optimization*, Computers & Structures, **85**(19-20), (2007), 1579–1588, DOI 10.1016/j.compstruc.2006.10.013.

33 **Camp C V**, *Design of Space Trusses Using Big Bang–Big Crunch Optimization*, Journal of Structural Engineering, **133**(7), (2007), 999–1008, DOI 10.1061/(ASCE)0733-9445(2007)133:7(999).

34 **Kaveh A, Mahdavi V R**, *Colliding Bodies Optimization method for optimum design of truss structures with continuous variables*, Advances in Engineering Software, **70**, (2014), 1–12, DOI 10.1016/j.advengsoft.2014.01.002.

35 **Li L J, Huang Z B, Liu F, Wu Q H**, *A heuristic particle swarm optimizer for optimization of pin connected structures*, Computers & Structures, **85**(7-8), (2007), 340–349, DOI 10.1016/j.compstruc.2006.11.020.

36 **Kaveh A, Talatahari S**, *A particle swarm ant colony optimization for truss structures with discrete variables*, Journal of Constructional Steel Research, **65**(8-9), (2009), 1558–1568, DOI 10.1016/j.jcsr.2009.04.021.

37 **Lingyun W, Mei Z, Guangming W, Guang M**, *Truss optimization on shape and sizing with frequency constraints based on genetic algorithm*, Computational Mechanics, **35**(5), (2005), 361–368, DOI 10.1007/s00466-004-0623-8.

38 **Construction AIOS**, *Manual of steel construction: allowable stress design*, American Institute of Steel Construction (AISC); Chicago (IL), 1989.

39 **Saka M P**, *Optimum design of pin-jointed steel structures with practical applications*, Journal of Structural Engineering, **116**(10), (1990), 2599–2620, DOI 10.1061/(ASCE)0733-9445(1990)116:10(2599).

40 **Hasançebi O, Çarbaş S, Doğan E, Erdal F, Saka M P**, *Performance evaluation of metaheuristic search techniques in the optimum design of real size pin jointed structures*, Computers & Structures, **87**(5-6), (2009), 284–302, DOI 10.1016/j.compstruc.2009.01.002.